

Electrochemical Study of the Herbicide Paraquat Based on a Graphene-Zinc Oxide Nanocomposite

Hua Liu¹, Maoqi Chen¹, Yi Lin¹ and Yanhong Liu^{2*}

¹ Department of Biomedical Engineering, Guangdong Pharmaceutical University, Guangzhou 510006, China

² Department of Endocrinology, The Second People's Hospital of Hengshui, Hengshui 053000, China

*E-mail: hswyliuyanhong@sina.com

Received: 24 May 2017 / *Accepted:* 22 June 2017 / *Published:* 13 August 2017

Detection of the herbicide paraquat (PQ) is of great significance in the field of agriculture. To detect PQ, this work proposed the fabrication of a new electrochemical sensor based on graphene oxide/ZnO nanorod (GR/ZnO)-modified graphite screen-printed electrodes (SPEs). SPEs were used since they are small, low-cost and versatile. The GR/ZnO-modified SPE was prepared by casting a nanocomposite of the GR/ZnO nanorods on the SPE surface. The two reduction DPV peaks of PQ were remarkably strengthened with GR/ZnO at -0.60 V and -1.00 V. The reduction peak currents of PQ on the GR/ZnO-modified SPE were linear under the optimal conditions (concentration range: 0.05 – 2 μ M), and the limit of detection (LOD) was 21 nM.

Keywords: Graphene oxide/ZnO nanorods; Screen-printed electrodes; Graphene; Electrochemical determination; Paraquat

1. INTRODUCTION

Paraquat (1,1'-dimethyl-4,4'-bipyridinium) (PQ) has been extensively used as a nonselective desiccant or herbicide for many different crops in more than 130 countries [1-3]. Nevertheless, PQ is highly toxic to plants and aquatic organisms due to its unfavourable properties [4]. PQ is significantly persistent in the environment and poses a great risk to the health of entire ecosystems since it is highly soluble in water (ca. 620 g/L at 25 °C) [5]. Additionally, PQ is extremely toxic to the health of humans and animals with an LD₅₀ of 35 mg/kg and 110 – 150 mg/kg, respectively, since it can be rapidly reduced. PQ ingestion can lead to kidney, heart, lung and liver failure in several days or several weeks and can possibly result in death up to 30 days after ingestion. It is most likely that those exposed to high concentrations of PQ will die. PQ is even associated with Parkinson's disease in farm workers since it can increase the formation of some cellular structures with harmful oxygen derivatives [6].

Timely elimination and accurate quantification of PQ in an individual's body are vital for the survival and recovery of patients. Hence, it is essential to develop an accurate and fast technique to detect PQ.

To detect PQ, multiple analytical strategies have recently been proposed, including spectrophotometry [7, 8], liquid chromatography [9-11], capillary electrophoresis [12] and gas chromatography/mass spectrometry [13]. As traditional techniques, liquid chromatography and spectrometry ordinarily entail a concentration procedure for LOD improvement, which could lead to damage to the specimens [14]. In addition, the other techniques are sophisticated and entail professional operators and labs as well as high-cost devices. In comparison, the appealing and facile method of electrochemistry could simplify the determination procedures and promote the response signals of the analytes [15, 16], especially for surface electrochemical methods [17].

Screen-printed electrodes (SPEs) have been used to miniaturize electrochemical analytical systems [18, 19]. SPEs are the best substitute for miniaturization due to their cost-effectiveness, convenient operation and high versatility [20, 21]. In addition, in contrast to glassy carbon electrodes (GCEs) and other traditional electrodes, SPEs make a cleaning procedure unnecessary [22]. SPEs are often integrated using nanoscale materials to enhance their electrochemical behaviour [23, 24].

In comparison with bare electrodes, modified electrodes are selective and sensitive, and they possess desirable electrocatalytic activities and low LODs. It has been widely acknowledged that electrodes modified by nanostructures (nanostructure metal oxides, Au nanoparticles, and carbon nanomaterials) can be used to promote the direct electron exchange of biomolecules [25-28]. ZnO nanostructures are better than other metal oxides, and they are the best candidate for the preparation of effective sensors due to their many advantages, including their promoted electron exchange, non-toxicity, large excitation binding energy (60 eV), and wide band gap (3.37 eV) [29, 30].

Graphene is a new one-atom thick planar sheet of sp^2 hybridized carbon atoms packed in a honeycomb lattice. This material has gained attention recently since it possesses a remarkable electrical conductivity, high specific surface area, and desirable charge carrier mobility [31-33]. Thus, the composites based on this material, such as graphene/ZnO, could potentially be proposed as new materials to modify electrodes and further improve the sensing sensitivity.

No work on the detection of paraquat with a GR/ZnO-modified SPE has been reported in previous literature. To detect paraquat, this work prepared and used a GR/ZnO (a nanocomposite)-based SPE, and neither specific reagents nor an electron transfer mediator were employed. The GR/ZnO-based SPE has multiple advantages, including no need for an electron transfer mediator, a wide linear dynamic range and a short operation time.

2. EXPERIMENTS

2.1. Chemicals

The GSPEs were commercially available from Italsens Co. The electrochemical experiments were carried out on an Autolab potentiostat/galvanostat, and the test conditions were controlled by the General Purpose Electrochemical System (GPES) software. The buffer solutions were synthesized from orthophosphoric acid and its salts (pH 2.0–9.0). All chemicals, including the paraquat, were commercially available from Sigma and were analytical reagent grade.

2.2. Synthesis of Graphene Oxide/ZnO Nanorods Nano Composite

Natural graphite flakes were used for the synthesis of graphene oxide nanosheets using a modified Hummers method. A mixture was obtained by dispersing 0.096 g of the reduced graphene oxide (RGO) in water (40 ml) with ultrasonication for 60 min, and the dispersion was then introduced into a ZnCl₂ (40 ml, 0.04 M) solution. Then, an ammonia solution was used to adjust the pH to 11.7. The terminal solution was kept at 95 °C for 4 h and centrifuged for 15 min at 15000 rpm to collect the precipitate. After washing three times with distilled water, the terminal product was dried in an oven for 4 h at 45 °C.

2.3. Preparation of the Electrode

The following steps describe the coating process of the original SPE using GR/ZnO. First, GR/ZnO (1 mg) was dispersed into an aqueous solution (1 mL) and ultrasonicated for 60 min to prepare a stock solution of GR/ZnO. This was followed by casting an aliquot (2 µL) of the prepared GR/ZnO suspension solution onto the SPE and keeping the solution on the SPE until the solvent evaporated at ambient temperature.

2.4. Characterizations

X-ray diffraction (XRD) was used to carry out the qualitative phase analysis of the electrocatalyst with a Philips XPERT PRO system, and Cu K α radiation ($\lambda = 0.15406$ nm) was used with an operating current and voltage of approximately 40 mA and 45 kV, respectively. An ESCALab 220i-XL electron spectrometer purchased from VG scientific was used to measure the X-ray photoelectron spectroscopy (XPS) data with 300 W Al K α radiation and a base pressure of approximately 3×10^{-9} mbar. The Raman analysis was carried out at room temperature using a Raman spectrometer (Renishaw InVia, UK) with a 514 nm laser light.

3. RESULTS AND DISCUSSION

The GR/ZnO composite nanostructures were characterized using the X-ray diffraction (XRD) profile in Fig. 1. The diffraction peaks of this composite were observed at 2θ values of 31.7°, 34.6°, 36.3°, 47.4°, 56.5°, 62.8°, 66.4°, 68.3° and 69.1°. These typical peaks could be ascribed to the (100), (002), (101), (102), (110), (103), (200), (112) and (201) planes along with the ZnO hexagonal wurtzite structure and corresponding to the standard ZnO peaks (JCPDS 36-1451) [34]. A broad and single diffraction peak was observed at $2\theta = 26.4^\circ$ for the as-prepared GR/ZnO nanostructures, which was ascribed to the (002) reflections of the graphitic carbon and to the GR. The XRD profiles did not show any typical peaks for ZnCl₂ or other impurities.

To study the defects, structure, and crystallization of the GR/ZnO composite, we used a Raman spectroscopy method for the investigation. The composite was characterized using the characteristic

Raman spectrum in Fig. 2. A D band and G band were observed at 1372 cm^{-1} and 1593 cm^{-1} , respectively, for the GR, as shown in Fig. 2A. Shifts to 1365 and 1598 cm^{-1} for the D and G bands were observed after the composite formed. These results showed that the D band and G band displayed a slight redshift of 7 cm^{-1} and a slight blueshift of 5 cm^{-1} , respectively, in the composite.

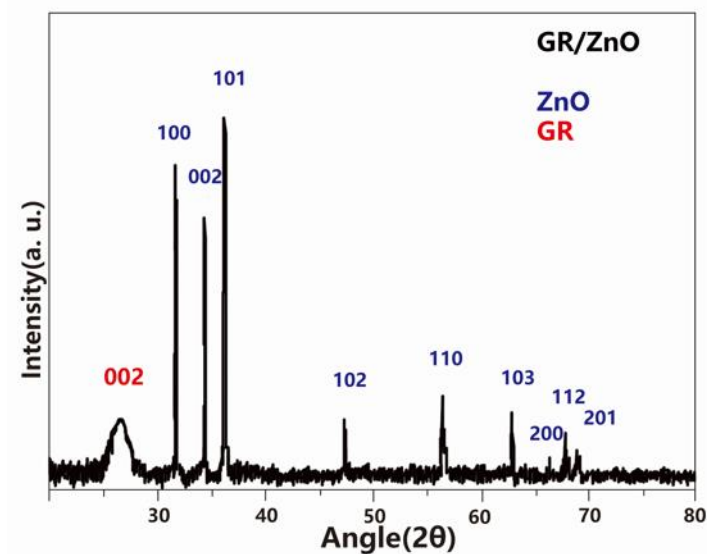


Figure 1. XRD profile of the as-prepared GR/ZnO composites.

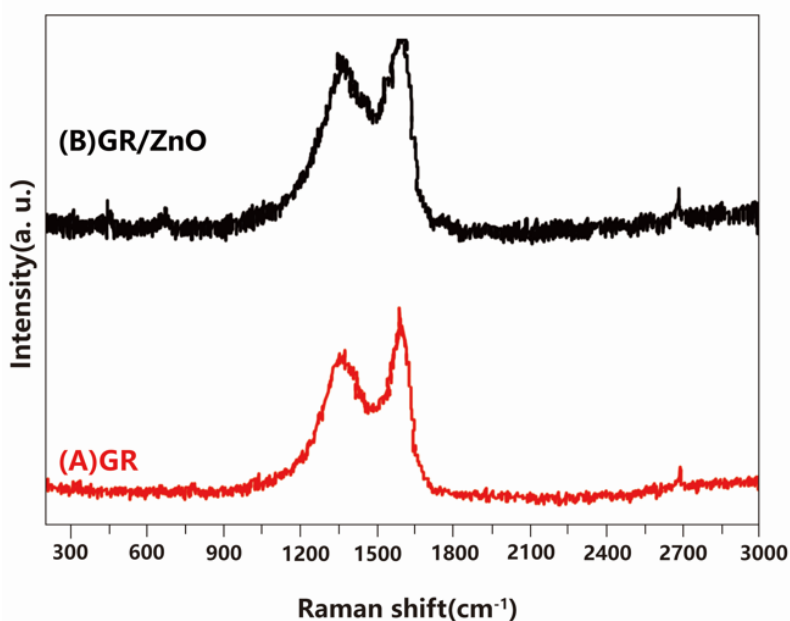


Figure 2. Raman characterization of (A) GR and (B) the GR/ZnO composite.

As indicated by the varying positions of the D, G and 2D bands of the GR and GR/ZnO, the GR strongly interacted with the ZnO in the composite via surface deposition or chemical bonding with the functional groups of graphene. The I_D/I_G (intensity ratio of the D and G bands) ratio was 0.94 and 1.11 for GR and the GR/ZnO composite, respectively. Therefore, an increase in the disorder was

indicated by the I_D/I_G increase, which was ascribed to the combination of the graphene layers of GR and the ZnO nanoparticles.

The XPS profiles were used to examine the chemical states and the surface composition based on the corresponding binding energies of the varying elements in the materials. The XPS profile of the GR/ZnO is shown in Fig. 3A, and the presence of O, C and Zn (dominant elements) at 5.10, 73.44 and 21.27, respectively, was indicated. The composite also showed an additional weak peak for N, which was ascribed to the incorporation of ammonia. C=O (288.3 eV), C–C (284.6 eV), and C–O (285.8 eV) appeared in the deconvoluted XPS C 1s profile (Fig. 3B) [35]. As shown in Fig. 3C, the Zn 2p core level regions were displayed in the XPS profile. A doublet was shown for the composite ca. 1045 and 1021.6 eV and was ascribed to the Zn 2p_{1/2} and 2p_{3/2} core levels, respectively. The O 1s region of the composite is shown in the XPS profile in Fig. 3D. Two distinct oxygen forms were displayed in the O 1s core-level spectrum. The lower binding energy at 529.8 eV corresponded to the Zn–O bonds of the wurtzite structure of ZnO [36]. The other peak at 532.1 eV corresponded to the OH groups absorbed on the ZnO nanoparticle surfaces [37].

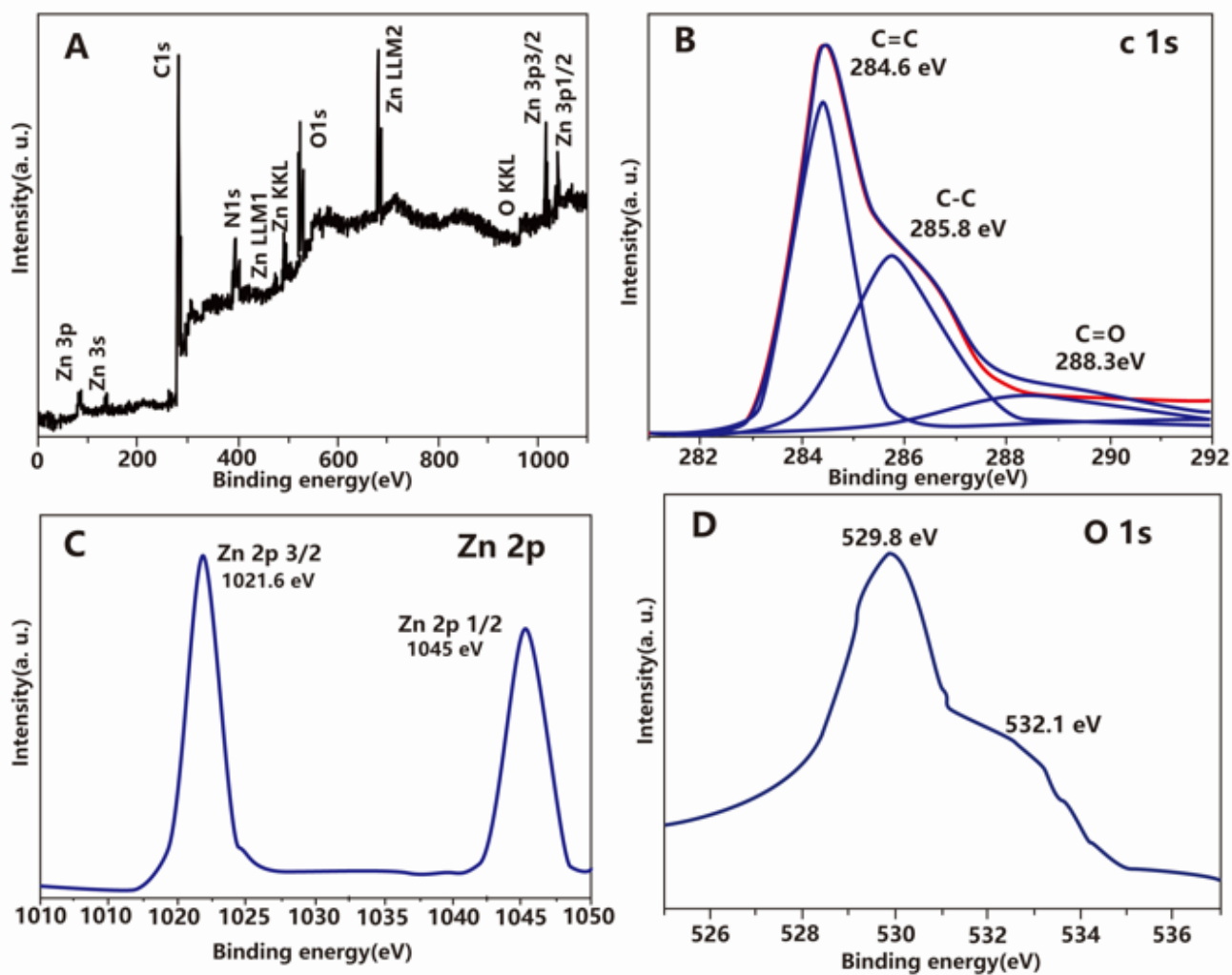
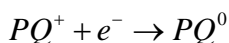
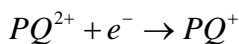


Figure 3. XPS profile: (A) a complete survey; (B) C 1s, (C) Zn 2p, and (D) O 1s core levels of the GR/ZnO composite.

To study the electrochemical performance of PQ on the modified SPEs, we used DPV for the investigation. The original SPE, the GR-modified SPE, the ZnO-modified SPE and the GR/ZnO modified-SPE in PBS were separately characterized after the addition of PQ (10 μ M; pH, 5.60) via the DPV profiles in Fig. 4. Obviously, the original SPE showed no reduction peaks. In addition, only a weak reduction peak (P1) at ca. -0.6 V was observed for the SPE in PBS after the addition of PQ (10 μ M). However, the other three SPEs showed P1 and another reduction peak ca. -1.0 V (P2), as shown in the DPV profiles. The two peaks mentioned above, P1 and P2, corresponded to the two redox couples [38].



Both of the response peaks (P1 and P2) for PQ on the modified SPEs were significantly more pronounced than the single peak (P1) observed on the original SPE, which suggested a remarkable enhancement in the features of the modified electrodes. In addition, the P1 potential was observed to shift positively in the range of -0.63 to -0.60 V, and the PQ peak current on the GR-modified GCE was observed to increase compared with the original SPE, which suggested that GR displayed a more desirable electrocatalytic activity compared to the SPE. Compared to the NGE-modified GCE, the P2 potential of the GR/ZnO-modified SPE was more positive. Additionally, compared to the GR-modified SPE, the GR/ZnO-modified SPE showed enhanced peak currents for P1 and P2, suggesting that a synergistic effect was present between ZnO and GR. In addition, compared to other the modified electrodes, the GR/ZnO-modified SPE showed PQ peak currents with larger DPV responses, which suggested a more rapid electron transfer and a higher specific surface area on the GR/ZnO.

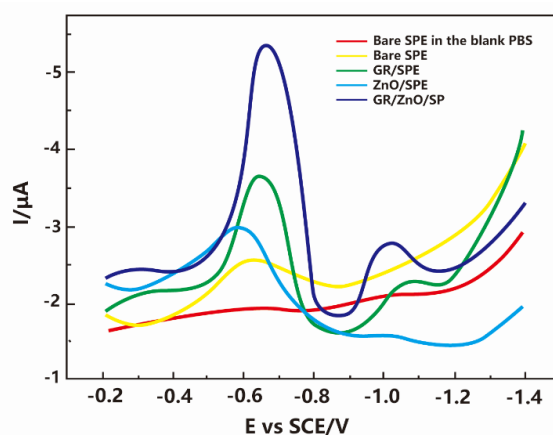


Figure 4. DPV profiles recorded on the original SPE in PBS compared with those on the original SPE, the GR-modified SPE, the ZnO-modified SPE and the GR/ZnO-modified SPE in PBS after the addition of PQ (10 μ M) at a scan rate of 50 mV/s.

Different amounts of GR/ZnO were used to determine the optimized behaviour of the GR/ZnO-modified SPE-based sensor for the electrochemical detection of PQ. To optimize the amount of GR/ZnO, varying dosages of the composite were used (0.10, 0.15, 0.20, 0.25 and 0.30 μ L) to fabricate 5 different GR/ZnO-modified SPEs. PQ (10 μ M) on varying electrodes in PBS was characterized via

the DPV profiles in Fig. 5A. Compared with the other 4 SPEs, the GR/ZnO (0.20 μL)-modified SPE showed a more pronounced response. The association of the GR/ZnO content with the intensities of the peak currents (P1 and P2) is directly displayed in Fig. 5B. An increase in the peak currents of P1 and P2 was observed as the GR/ZnO amount increased in the range of 0.10 - 0.20 μL , whereas a decrease was observed as the GR/ZnO amount increased in the range of 0.20 - 0.30 μL . Therefore, 0.20 μL was selected as the optimized amount of GR/ZnO.

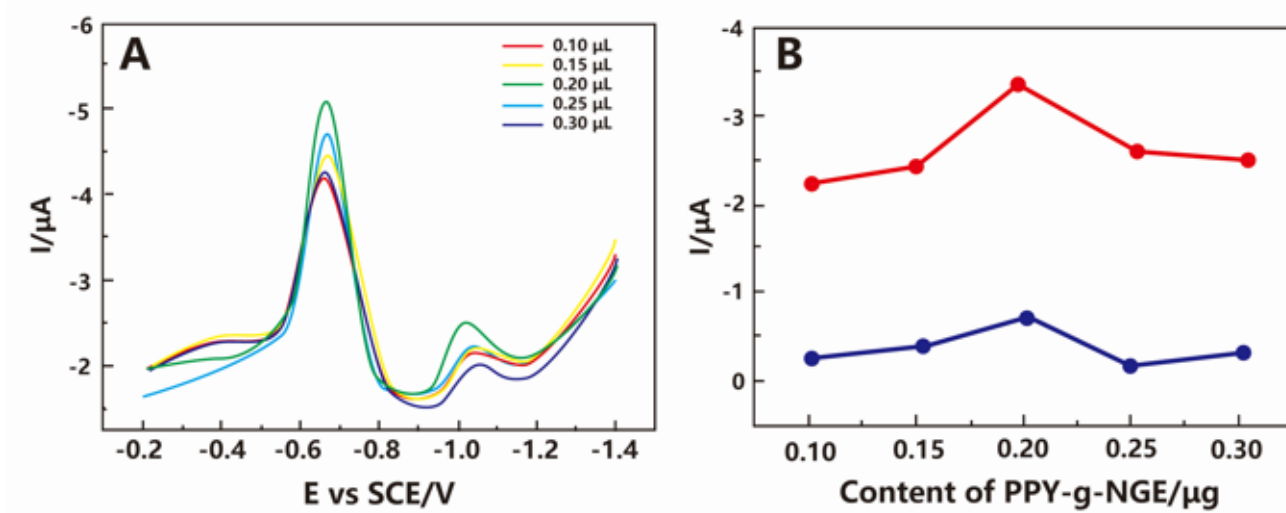


Figure 5. (A) DPV profiles of PQ (10 μM) in PBS (pH, 5.60) on the GR/ZnO-modified SPE with GR-modified ZnO (in varying amounts): 0.10, 0.15, 0.20, 0.25, and 0.30 μL . (B) Effect of the content of the GR-modified ZnO on the peak currents of PQ (10 μM).

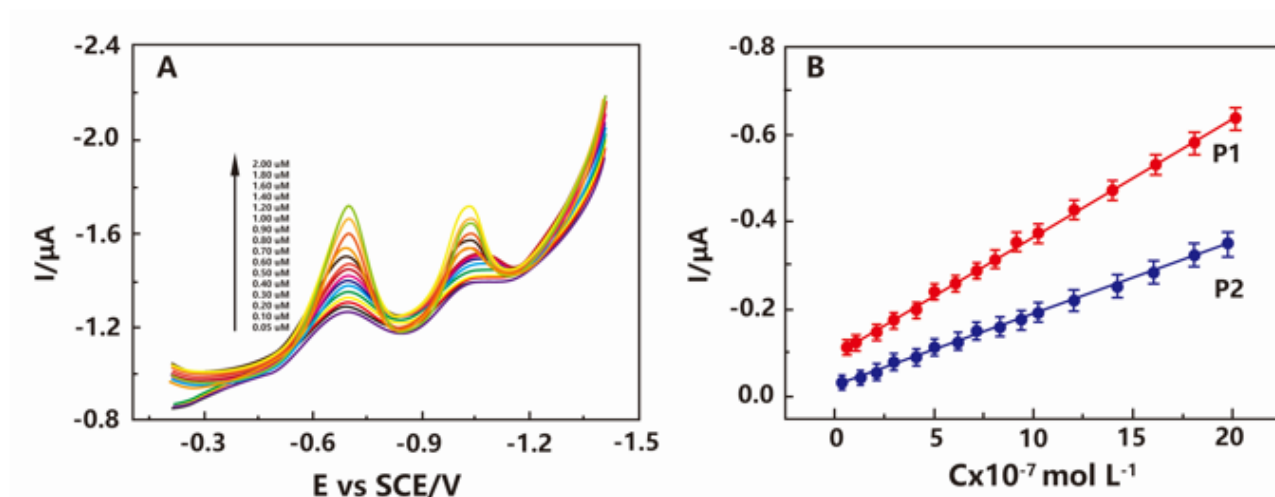


Figure 6. (A) The DPV profiles of varying concentrations of PQ on the GR/ZnO-modified SPE (0.05, 0.10, 0.20, 0.30, 0.40, 0.50, 0.60, 0.70, 0.80, 0.90, 1.00, 1.20, 1.40, 1.60, 1.80, and 2.00 μM). (B) Dependence of the Ipc on the concentration of PQ.

The electrochemical PQ detection was carried out on the GR/ZnO-modified SPE under the aforementioned optimal conditions. Varying concentrations of PQ (50 nM - 2 μ M) on the GR/ZnO-modified SPE were characterized via the DPV profiles in Fig. 6A. As the concentration increased, a proportional increase in the cathodic peak currents of P1 at -0.69 V and P2 at -1.03 V was observed. Subsequently, the calibration lines were drawn based on the peak currents shown in Fig. 6B. The LODs, which were calculated at a ratio of sound to noise of 3, were 21 nM and 34 nM for P1 and P2, respectively. As displayed in Table 1, the LOD of the GR/ZnO-modified SPE was lower compared with several previously proposed electrodes, indicating that the GR/ZnO-modified SPE is applicable for the PQ determination.

Moreover, the obtained GR/ZnO-modified SPE was utilized to analyse trace amounts of PQ in three soil samples collected from cultivated land as real environmental samples. The results of the carbendazim content determination in these two soil samples are shown in Table 2. As shown, the GR/ZnO-modified SPE had an excellent performance for PQ detection in the soil samples.

Table 1. Comparison of varying electrodes toward the PQ detection.

Electrode	Linear range (μ M)	Detection of limit (μ M)	Reference
PPY-NGE/GCE	0.05–2	0.041	[39]
Bismuth-film electrode	0.66–48	0.093	[40]
AuNPs/DNA/GE	0–100	1.3	[1]
MWCNTs-DHP/GCE	0.20–1.70	0.026	[2]
Microelectrodes	1-166	0.45	[41]
DNA-modified carbon ionic liquid electrode	0.05-70	0.036	[42]
Nafion film coated glassy carbon electrode	10-100	1	[43]
GR/ZnO/SPE	0.05–2	0.021	This work

Table 2. The contents and recoveries of GR/ZnO modified SPE for PQ determination in PQ (n=3).

Sample	Added (μ M)	Found (μ M)	ELISA result (μ M)	Recovery (%)	RSD (%)
1	0.40	0.398	0.390	99.5	4.3
2	0.80	0.807	0.808	100.88	1.8
3	1.60	1.605	1.594	100.31	2.7

4. CONCLUSIONS

This study reported the fabrication of a new sensor for ultrasensitive PQ detection, and the SPEs were modified using a GR/ZnO-nanorod nanocomposite. In comparison with the ZnO-modified SPE and GR-modified SPE, the proposed GR/ZnO-modified SPE showed remarkable electrocatalytic activity and electrochemical behaviour towards the redox reactions of PQ. Both the PQ peak currents

obtained on the proposed electrode under the optimal conditions were linear in the range 0.05–2 μM , and a LOD of 21 nM was obtained.

ACKNOWLEDGEMENTS

This work has been supported by the Science and Technology Plan of Guangdong Province (Grant No. 2012B031000018) .

References

1. J. Ribeiro, C. Carreira, H. Lee, F. Silva, A. Martins and C. Pereira, *Electrochimica Acta*, 55 (2010) 7892.
2. L. Garcia, L. Figueiredo-Filho, G. Oliveira, O. Fatibello-Filho and C. Banks, *Sensors and Actuators B: Chemical*, 181 (2013) 306.
3. H. El Harmoudi, M. Achak, A. Farahi, S. Lahrich, L. El Gaini, M. Abdennouri, A. Bouzidi, M. Bakasse and M. El Mhammedi, *Talanta*, 115 (2013) 172.
4. C. Infante, A. Morales-Rubio, M. de La Guardia and F. Rocha, *Talanta*, 75 (2008) 1376.
5. M. El Mhammedi, M. Bakasse, R. Bachirat and A. Chtaini, *Food Chemistry*, 110 (2008) 1001.
6. C. Tanner, F. Kamel, G. Ross, J. Hoppin, S. Goldman, M. Korell, C. Marras, G. Bhudhikanok, M. Kasten and A. Chade, *Environ. Health Perspect.*, 119 (2011) 866.
7. M. Rai, J. Das and V. Gupta, *Talanta*, 45 (1997) 343.
8. F. Maya, J. Estela and V. Cerdà, *Talanta*, 85 (2011) 588.
9. C. Fuke, T. Arao, Y. Morinaga, H. Takaesu, K. Ameno and T. Miyazaki, *Legal Medicine*, 4 (2002) 156.
10. M. Brunetto, A. Morales, M. Gallignani, J. Burguera and M. Burguera, *Talanta*, 59 (2003) 913.
11. M. Ibanez, Y. Picó and J. Manes, *Journal of Chromatography A*, 728 (1996) 325.
12. E. Mallat, C. Barzen, R. Abuknesha, G. Gauglitz and D. Barcelo, *Anal. Chim. Acta.*, 427 (2001) 165.
13. N. Posecion, E. Ostrea and D. Bielawski, *Journal of Chromatography B*, 862 (2008) 93.
14. A. Walcarius and L. Lamberts, *Journal of Electroanalytical Chemistry*, 406 (1996) 59.
15. T. Drummond, M. Hill and J. Barton, *Nature Biotechnology*, 21 (2003) 1192.
16. F. Patolsky, A. Lichtenstein and I. Willner, *Nature Biotechnology*, 19 (2001) 253.
17. G. Liang, T. Li, X. Li and X. Liu, *Biosensors and Bioelectronics*, 48 (2013) 238.
18. K. Chan, H. Lim, N. Shams, S. Jayabal, A. Pandikumar and N. Huang, *Materials Science and Engineering: C*, 58 (2016) 666.
19. F. Arduini, C. Zanardi, S. Cinti, F. Terzi, D. Moscone, G. Palleschi and R. Seeber, *Sensors and Actuators B: Chemical*, 212 (2015) 536.
20. C. Foster, J. Metters, D. Kampouris and C. Banks, *Electroanalysis*, 26 (2014) 262.
21. M. Chatzipetrou, F. Milano, L. Giotta, D. Chirizzi, M. Trotta, M. Massaouti, M. Guascito and I. Zergioti, *Electrochemistry Communications*, 64 (2016) 46.
22. N. Lezi, A. Economou, J. Barek and M. Prodromidis, *Electroanalysis*, 26 (2014) 766.
23. X. Zhu, X. Niu, H. Zhao and M. Lan, *Sensors and Actuators B: Chemical*, 195 (2014) 274.
24. M. Asadollahi-Baboli and A. Mani-Varnosfaderani, *Measurement*, 47 (2014) 145.
25. M. Yola, N. Atar, Z. Üstündağ and A. Solak, *Journal of Electroanalytical Chemistry*, 698 (2013) 9.
26. H.M. Moghaddam, H. Beitollahi, S. Tajik, I. Sheikshoaie and P. Biparva, *Environmental Monitoring and Assessment*, 187 (2015) 407.
27. V. Gupta, M.L. Yola, N. Atar, Z. Üstündağ and A. Solak, *Journal of Molecular Liquids*, 191 (2014) 172.
28. M. Hasheminejad and A. Nezamzadeh-Ejehieh, *Food Chemistry*, 172 (2015) 794.
29. V. Gupta, N. Atar, M. Yola, Z. Üstündağ and L. Uzun, *Water. Res.*, 48 (2014) 210.

30. K. Rawat, A. Sharma, P.R. Solanki and H. Bohidar, *Electroanalysis*, 27 (2015) 2448.
31. M. Yola, V. Gupta, T. Eren, A. Şen and N. Atar, *Electrochimica Acta*, 120 (2014) 204.
32. V. Gupta, M. Yola, M. Qureshi, A. Solak, N. Atar and Z. Üstündağ, *Sensors and Actuators B: Chemical*, 188 (2013) 1201.
33. M. Yola, N. Atar, T. Eren, H. Karimi-Maleh and S. Wang, *RSC Advances*, 5 (2015) 65953.
34. C. Hou, Q. Zhang, H. Wang and Y. Li, *Journal of Materials Chemistry*, 21 (2011) 10512.
35. O. Akhavan and E. Ghaderi, *ACS Nano*, 4 (2010) 5731.
36. J. Das, S. Pradhan, D. Sahu, D. Mishra, S. Sarangi, B. Nayak, S. Verma and B. Roul, *Physica B: Condensed Matter*, 405 (2010) 2492.
37. H. Zhou and Z. Li, *Mater. Chem. Phys.*, 89 (2005) 326.
38. P. Monk, C. Turner and S. Akhtar, *Electrochimica acta*, 44 (1999) 4817.
39. J. Li, W. Lei, Y. Xu, Y. Zhang, M. Xia and F. Wang, *Electrochimica Acta*, 174 (2015) 464.
40. L. de Figueiredo-Filho, V. dos Santos, B. Janegitz, T. Guerreiro, O. Fatibello-Filho, R. Faria and L. Marcolino-Junior, *Electroanalysis*, 22 (2010) 1260.
41. D. De Souza and S. Machado, *Anal. Chim. Acta.*, 546 (2005) 85.
42. N. Mai, X. Liu, W. Wei, S. Luo and W. Liu, *Microchim. Acta.*, 174 (2011) 89.
43. T. Lu and I. Sun, *Talanta*, 53 (2000) 443.

© 2017 The Authors. Published by ESG (www.electrochemsci.org). This article is an open access article distributed under the terms and conditions of the Creative Commons Attribution license (<http://creativecommons.org/licenses/by/4.0/>).